

Phase transition studied by ^7Li nuclear magnetic resonance in LiXSO_4 ($X = \text{K}, \text{Rb}, \text{Cs}$ and NH_4) single crystals

This article has been downloaded from IOPscience. Please scroll down to see the full text article.

2000 J. Phys.: Condens. Matter 12 9293

(<http://iopscience.iop.org/0953-8984/12/44/310>)

View [the table of contents for this issue](#), or go to the [journal homepage](#) for more

Download details:

IP Address: 171.66.16.221

The article was downloaded on 16/05/2010 at 06:57

Please note that [terms and conditions apply](#).

Phase transition studied by ^7Li nuclear magnetic resonance in LiXSO_4 ($X = \text{K}, \text{Rb}, \text{Cs}$ and NH_4) single crystals

Ae Ran Lim^{†||}, Sung Ho Choh[‡] and Se-Young Jeong[§]

[†] Department of Physics, Jeonju University, Jeonju 560-759, Korea

[‡] Department of Physics, Korea University, Seoul 136-701, Korea

[§] Department of Physics, Pusan National University, Pusan 609-735, Korea

E-mail: aeranlim@hanmail.net

Received 15 February 2000, in final form 15 August 2000

Abstract. The temperature dependences of ^7Li nuclear magnetic resonance in LiXSO_4 ($X = \text{K}, \text{Rb}, \text{Cs},$ and NH_4) single crystals grown by the slow evaporation method have been investigated by employing a Bruker FT NMR spectrometer. From the experimental data, the nuclear quadrupole constant, the asymmetry parameter and the principal axes of the EFG tensor were determined, and the results were compared with the crystal structure. The temperature dependences of the quadrupole parameters were explained with a single torsional mode of the Li–O bond by the Bayer theory. All the LiO_4 tetrahedra in four different crystals showed torsional motion about the X -axis of the EFG tensor. Based on these results, the differences in atomic weight of X in the LiXSO_4 single crystals are responsible for the differences in the torsional angular frequencies.

1. Introduction

The increasing number of studies being performed on the physical properties of LiXSO_4 ($X = \text{K}, \text{Rb}, \text{Cs}$ and NH_4) single crystals are largely owing to its excellent optical quality. These crystals have previously been investigated by means of x-ray diffraction [1–15], Raman spectroscopy [16–28], EPR [29–41], NMR [42–58] and optical properties [59–64]. Also, these materials have ferroelastic properties at low temperatures, as confirmed by stress–strain hysteresis results [65–68] and Aizu classification [69].

In this paper, we reviewed results of the ^7Li nuclear magnetic resonance (NMR) in LiXSO_4 ($X = \text{K}, \text{Rb}, \text{Cs}$ and NH_4) single crystals grown by the slow evaporation method. The quadrupole coupling constant, e^2qQ/h , the asymmetry parameter, η , and the direction of the principal axes of the electric field gradient (EFG) tensor of ^7Li ($I = 3/2$) in LiXSO_4 single crystals were determined as a function of temperature. The temperature dependences of the quadrupole parameters can be discussed with a single torsional frequency of the Li–O ion in the LiO_4 tetrahedron. We found for the first time that the differences in the atomic weight of the alkali ion in each single crystal are affected by the torsional frequency.

2. Crystal structure

These complex sulphates with the composition LiXSO_4 ($X = \text{K}, \text{Rb}, \text{Cs}$ and NH_4), where X represents an alkali ion, have structures which are based on the LiO_4 tetrahedron. The lithium

^{||} Author to whom all correspondence should be addressed.

Table 1. The bond lengths for LiO₄ tetrahedra in the LiXSO₄ (X = K, Rb, Cs and NH₄) single crystals.

LiKSO ₄		LiRbSO ₄		LiCsSO ₄		LiNH ₄ SO ₄	
Li–O	1.909 Å	Li–O	1.891 Å	Li–O	1.849 Å	Li–O	1.891 Å
Li–O	1.923 Å	Li–O	1.913 Å	Li–O	1.954 Å	Li–O	1.889 Å
Li–O	1.923 Å	Li–O	1.950 Å	Li–O	1.904 Å	Li–O	1.979 Å
Li–O	1.923 Å	Li–O	1.928 Å	Li–O	1.954 Å	Li–O	1.899 Å

Table 2. The structures of LiXSO₄ (X = K, Rb, Cs and NH₄) single crystals at room temperature.

	LiKSO ₄	LiRbSO ₄	LiCsSO ₄	LiNH ₄ SO ₄
Structure	hexagonal	monoclinic	orthorhombic	orthorhombic
Space group	<i>P</i> 63	<i>P</i> 21/ <i>n</i>	<i>P</i> <i>cmn</i>	<i>P</i> <i>mnn</i>
Lattice constant	<i>a</i> = 5.147 Å <i>c</i> = 8.633 Å	<i>a</i> = 5.288 Å <i>b</i> = 9.105 Å <i>c</i> = 8.731 Å <i>γ</i> = 90.09°	<i>a</i> = 5.456 Å <i>b</i> = 9.456 Å <i>c</i> = 8.820 Å	<i>a</i> = 5.28 Å <i>b</i> = 9.14 Å <i>c</i> = 8.786 Å

ion is surrounded by tetrahedrally coordinated oxygens. The bond lengths for LiO₄ tetrahedra are given in table 1. The structures of the LiXSO₄ single crystals are summarized in table 2. The lattice constants and crystal structures are similar to each other, while the phase transition temperatures are absolutely different.

3. Experimental procedure

LiXSO₄ (X = K, Rb, Cs and NH₄) single crystals were grown by slow evaporation from an aqueous solution of equimolar amounts of Li₂SO₄ · 4H₂O and X₂SO₄ (X = K, Rb, Cs and NH₄). These single crystals were transparent and colourless. The orientations of the crystal axes were determined by an optical polarizing microscope and the x-ray Laue method. The angular dependence of the NMR spectra was measured for rotations of the crystals around the crystallographic axes *c*, *a* and *b*.

Nuclear magnetic resonance signals of ⁷Li in LiXSO₄ single crystals were measured using a Bruker MSL 200 FT NMR spectrometer at the Korea Basic Science Institute in Seoul. The static magnetic field was 4.7 T and the central rf frequency was set at $\omega/2 = 77.777$ MHz.

4. Experimental results and analysis

4.1. ⁷Li NMR in LiKSO₄

The crystal structure of LiKSO₄ is hexagonal with the space group *P*63 (C66) and two formula units per cell at room temperature [10]. At lower temperatures, LiKSO₄ undergoes two phase transitions: phase I to phase II at 201 K and phase II to phase III at 190 K. Near 201 K [6], LiKSO₄ transforms from hexagonal phase to either a hexagonal phase [9] or a trigonal phase [17, 59]. Phase III, below 190 K, has been observed to be either orthorhombic [9, 18] or monoclinic [74]. In addition, LiKSO₄ undergoes at least two phase transitions above room temperature: at about 708 and 943 K [70, 71]. The structures of the high-temperature phases are not yet well established. At 708 K the crystal undergoes a structural phase transition, probably to the orthorhombic phase. The second phase transition, most likely to the hexagonal phase, is observed at 943 K. The phase between 708 and 943 K is known to be ferroelastic [72].

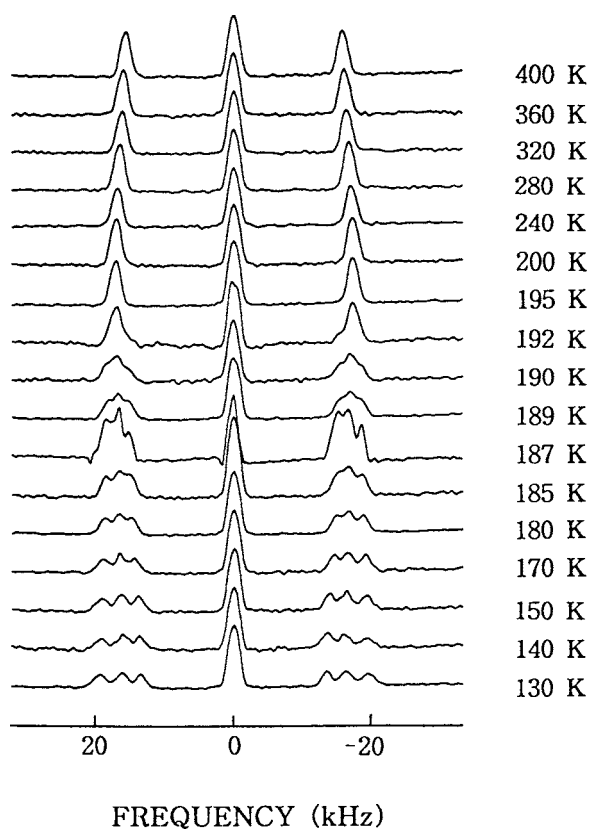


Figure 1. The temperature dependence of the ${}^7\text{Li}$ NMR spectra in an LiKSO_4 crystal.

The ${}^7\text{Li}$ NMR spectra were measured in the temperature range of 130 to 400 K. The spectrum displayed only three lines for all orientations of the crystal above 190 K, as shown in figure 1. The splitting of ${}^7\text{Li}$ resonance lines slightly changed in the range above 190 K, which includes the phase transition from I to II. Above phase II, maximum separation of the resonance lines due to the quadrupole interaction was observed when the magnetic field was applied along the c -axis of the crystal. This direction was determined to be the Z -axis of the EFG tensor. From these NMR results, the quadrupole coupling constant of ${}^7\text{Li}$, $e^2qQ/h = 25$ kHz, and the asymmetry parameter, $\eta = 0.15$, were determined at room temperature [50]. These values proved to be non-axially symmetric, consistent with the fact that the coordination of the lithium ion surrounded by oxygen atoms did not form a perfectly regular tetrahedron. Also, because there was no change in the ${}^7\text{Li}$ NMR spectrum during the phase transition from I to II at 201 K, we could not distinguish between the trigonal and hexagonal space groups proposed for the phase II.

The ${}^7\text{Li}$ NMR line splits into three lines at the transition point of 190 K as shown in figure 1. The ${}^7\text{Li}$ NMR spectra below 190 K showed only continuous changes in the quadrupole splittings. From these results, the NMR parameters were obtained. These had the same magnitude of quadrupole coupling constants and asymmetry parameters for resonance lines of each of the three sets, but had different orientations, and were rotated with respect to each other by 120° around the c -axis. These factors are due to the existence of three kinds of ferroelastic domain. Recently, the structure of the ferroelastic domain is has been discussed in terms of

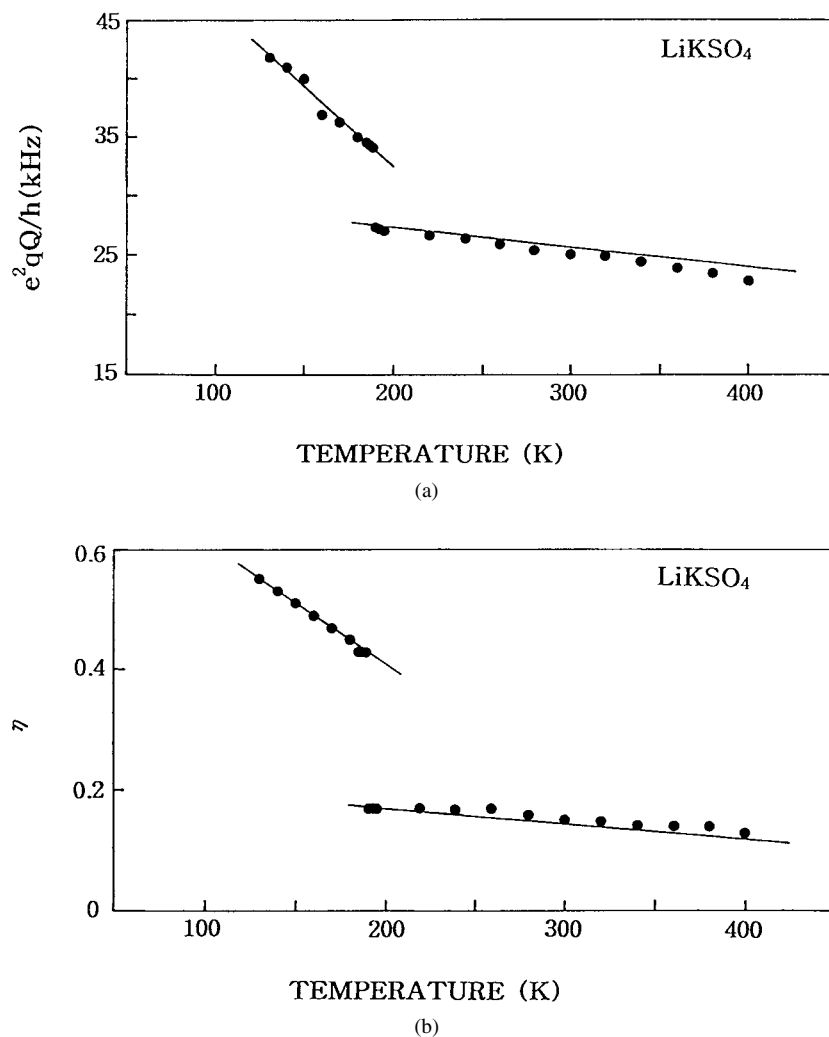


Figure 2. Temperature dependence of the nuclear quadrupole coupling constant and asymmetry parameter for ^7Li NMR in LiKSO_4 crystal.

^7Li and ^{39}K NMR results [73]. The principal axes of the ^7Li EFG tensor below 190 K are the same as when it is at room temperature. The principal axes of the Li ion are consistent with the crystallographic axes [51].

The e^2qQ/h and η for the ^7Li nucleus in the temperature range of 130–400 K is shown in figure 2. At the transition point of 190 K, the parameters of the ^7Li NMR change abruptly, demonstrating a change in the lithium site symmetry, and the asymmetry parameter η changes from 0.17 above 190 K to 0.44 below 190 K. The quadrupole coupling constant jumps to a value of 34 kHz at the transition point of 190 K. This means that the phase II to III transition is first order. We attempted to explain the temperature dependence of the e^2qQ/h and η for ^7Li in terms of a torsional oscillation of the Li–O ion [74, 75]. The values of e^2qQ/h and η above and below 190 K were found to decrease almost linearly as a function of increasing temperature; e^2qQ/h and η decrease with increasing temperature for this torsional motion about the X-axis. The moment of inertia calculated for the LiKSO_4 crystal structure is $I_x = 2.73 \times 10^{-45} \text{ kg m}^2$

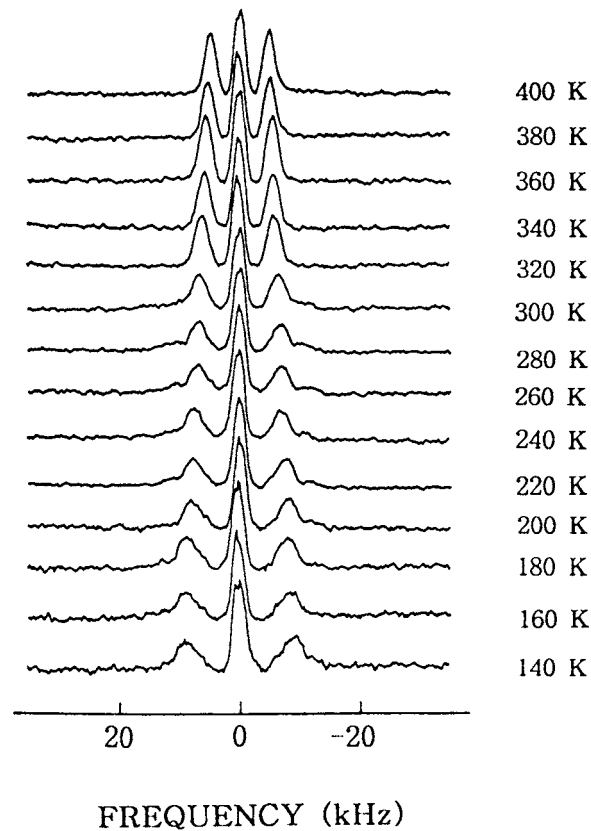


Figure 3. The temperature dependence of the ${}^7\text{Li}$ NMR spectra in the LiRbSO_4 crystal.

for the X -axis. The solid lines above and below 190 K in figure 2 are the predicted values of e^2qQ/h and η for ${}^7\text{Li}$ with $w_x = 3.92 \times 10^{13} \text{ rad s}^{-1}$ and $w_x = 1.36 \times 10^{13} \text{ rad s}^{-1}$, respectively.

4.2. ${}^7\text{Li}$ NMR in LiRbSO_4

Studies on the successive phase transitions in LiRbSO_4 single crystal have been conducted and reported by several groups [76–80]. It has been discovered that LiRbSO_4 crystals undergo successive transitions at 439, 458, 475 and 477 K [76, 77]. These phases have been called I–V in the order of descending temperature. Phases I and V are paraelectric [77]. Phases II and III are ferroelectric and antiferroelectric, respectively [81]. Microscopic observations indicate that phases IV and V are monoclinic, and that the crystal structure is orthorhombic above 458 K [80]. Ferrielectricity has been found in phase IV between 439 and 458 K [77].

The rotation patterns of Li were measured in the three crystallographic planes at room temperature. Because the resonance frequency of the central line is almost constant and the splitting between adjacent lines is equal, the first-order perturbation of H_Q to H_Z is sufficient for analysis. By the maximum separation of the resonance line, the c -axis of the crystal is found to be the Z -axis of the EFG tensor. The quadrupole parameters were determined by a least-squares fit using the experimental data; the quadrupole coupling constant $e^2qQ/h = 20.4 \text{ kHz}$ and asymmetry parameter $\eta = 0$ were determined at room temperature [53].

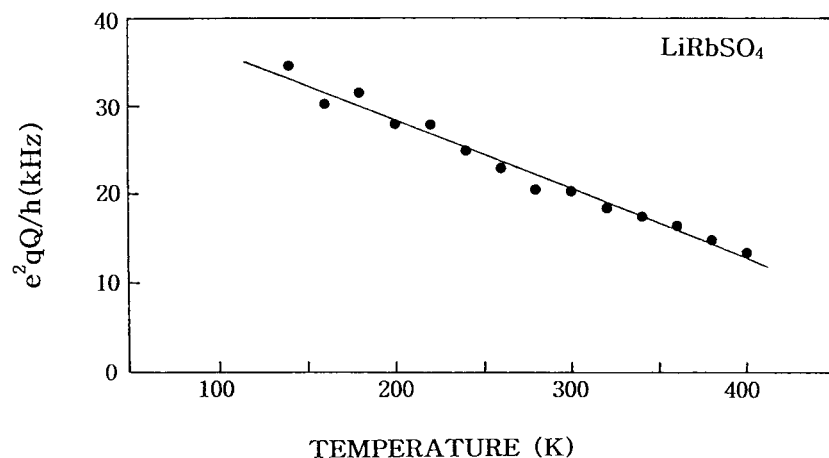


Figure 4. Temperature dependence of the nuclear quadrupole coupling constant for ${}^7\text{Li}$ NMR in the LiRbSO_4 crystal.

The resonance spectra were measured in the range of 140 to 400 K as shown in figure 3. The line splitting between the central and satellite lines is found to decrease as the temperature increases. Also, the intensity of the resonance line is found to be increased as the temperature increases. The temperature dependence of e^2qQ/h for ${}^7\text{Li}$ in the LiRbSO_4 single crystal is shown in figure 4. The value of e^2qQ/h was found to decrease almost linearly as a function of increasing temperature. The temperature dependence of e^2qQ/h can be explained by the torsional motion about the X -axis. The moment of inertia, $I_x = 2.48 \times 10^{-45} \text{ kg m}^2$ for the X -axis, was calculated from the bond length of table 1. The inertia moment is calculated by the nearest four oxygen ions. The solid lines in figure 4 are the predicted values of e^2qQ/h for ${}^7\text{Li}$ with $w_x = 8.30 \times 10^{12} \text{ rad s}^{-1}$. Therefore, the Bayer–Wang theory can satisfactorily explain our data for the temperature range 140–400 K.

4.3. ${}^7\text{Li}$ NMR in LiCsSO_4

LiCsSO_4 single crystals undergo a transition from the paraelastic phase with orthorhombic structure at room temperature to the ferroelastic phase with monoclinic structure below $T_c = 202 \text{ K}$ [9, 82].

The ${}^7\text{Li}$ NMR spectra were measured in the temperature range of 140 to 400 K, as shown in figure 5. Above T_c , the ${}^7\text{Li}$ NMR spectrum showed three lines for all orientations of the magnetic field, while two sets of ${}^7\text{Li}$ NMR spectra were recorded below T_c . From the rotation patterns of ${}^7\text{Li}$ NMR spectra in the three crystallographic planes, the nuclear quadrupole coupling constant and asymmetry parameter of ${}^7\text{Li}$ in an LiCsSO_4 crystal were determined as 22.35 kHz and 0.68 at room temperature. The satellite resonance lines did not show the extrema along the crystallographic axis. Based on these experimental results, we can conclude that the principal axes of the Li ion are not parallel to the crystallographic axes. The EFG tensor of ${}^7\text{Li}$ was found to be asymmetric. The direction of the principal EFG tensor at 300 K is represented with the Eulerian angles $\Phi = 90^\circ$, $\Theta = 20^\circ$ and $\Psi = 0^\circ$ [54].

At the transition point of 200 K, the ${}^7\text{Li}$ NMR line splits into two sets. The rotation patterns of the ${}^7\text{Li}$ NMR spectra are measured in the ab -, bc - and ca -plane below 200 K. The obtained results can be explained by the existence of two kinds of ferroelastic domain, rotated with respect to each other by 120° around the c -axis. Below 200 K, the ${}^7\text{Li}$ NMR spectra showed

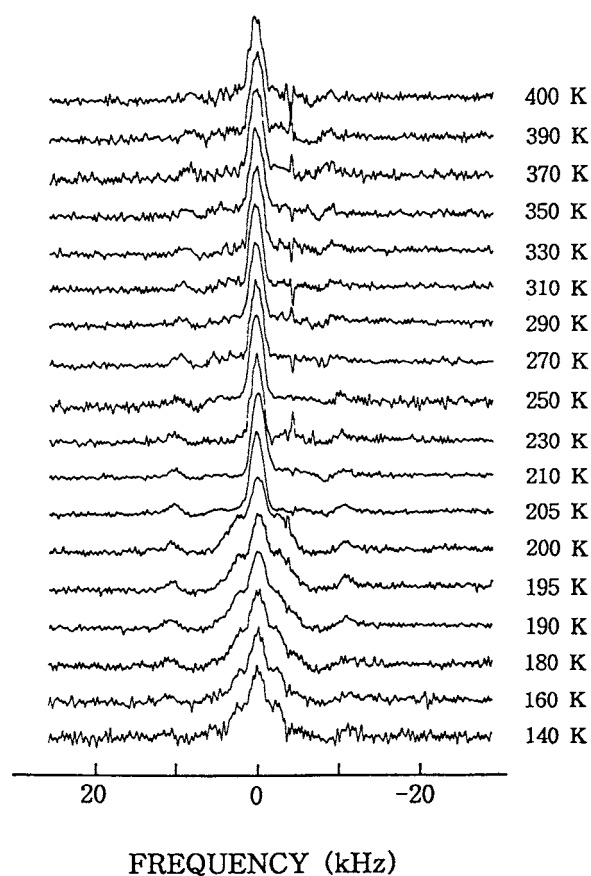


Figure 5. The temperature dependence of the ${}^7\text{Li}$ NMR spectra in the LiCsSO_4 crystal.

only continuous quantitative changes in the quadrupole splittings, without any other abrupt changes. The ${}^7\text{Li}$ NMR spectra demonstrated the occurrence of a phase transition at 200 K, which is connected with a lowering of the Li^+ site symmetry and formation of two kinds of ferroelastic domain. The experimental data show that the principal axes of the ${}^7\text{Li}$ EFG tensor below T_c are not the same as those above T_c . This means that the phase transition is second order. The principal X -, Y - and Z -axes are found to lie along the Eulerian angles $\Phi = 70^\circ$, $\Theta = 15^\circ$ and $\Psi = 35^\circ$. The nuclear quadrupole coupling constant and asymmetry parameter of ${}^7\text{Li}$ in an LiCsSO_4 crystal were determined to be 26.90 kHz and 0.79 at 180 K [54].

The temperature dependences of e^2qQ/h and η in the temperature range of 140–400 K are shown in figure 6. For the torsional motion about the X -axis, both e^2qQ/h and η decrease with increasing temperature. The Mathematica package was used to simulate the variations of e^2qQ/h and η . We controlled sensitivity variations of w_x for the slopes of the e^2qQ/h and η obtained from our NMR experimental results. The straight line in figure 6 is the prediction of e^2qQ/h and η for ${}^7\text{Li}$ with $I_x = 1.67 \times 10^{-45}$ kg m² and $w_x = 4.50 \times 10^{12}$ rad s⁻¹.

4.4. ${}^7\text{Li}$ NMR in LiNH_4SO_4

LiNH_4SO_4 single crystals undergo two phase transitions [42, 83, 84] with T_{c1} at 459 K and T_{c2} at approximately 283 K. These take the crystal from the orthorhombic high temperature phase of space group D_{2h}^{16} ($z = 4$) [85] to another orthorhombic phase, space group C_{2v}^9 [86],

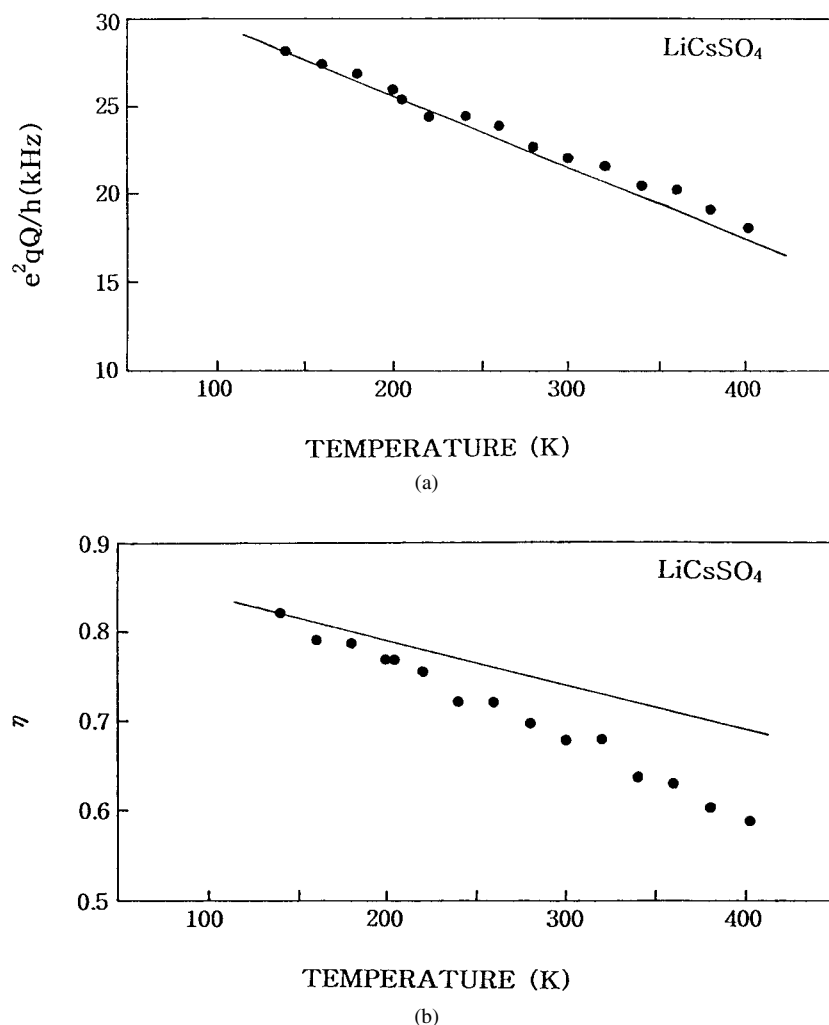


Figure 6. Temperature dependence of the nuclear quadrupole coupling constant and asymmetry parameter for ${}^7\text{Li}$ NMR in the LiCsSO_4 crystal.

and then transform it further to a monoclinic phase, space group C_{2h}^5 [87]. Three phases of LiNH_4SO_4 can be distinguished: phase I for $T > 459$ K, phase II for $283 \text{ K} < T < 459$ K, and phase III for $T < 283$ K. It has been established that the phase transition from phase II to III is of the first order, while that from phase I to II is of the second order [43].

In the temperature range of 170 to 400 K, the ${}^7\text{Li}$ NMR spectra were measured as shown in figure 7. A ${}^7\text{Li}$ NMR spectrum consists of only three lines for all orientations of the crystal above T_{c2} ($=283$ K). From these NMR results, the quadrupole coupling constant, $e^2qQ/h = 25$ kHz, and asymmetry parameter, $\eta = 0.22$, were obtained at room temperature. The EFG tensor of ${}^7\text{Li}$ was found to be non-axially symmetric. At room temperature, the satellite resonance lines showed neither maximum nor minimum separation along the crystallographic axes. Thus, we can conclude that the principal axes of the EFG tensor are not parallel to the crystallographic axes. The directions of the principal EFG tensors at room temperature are represented with the Eulerian angles $\Phi = 80^\circ$, $\Theta = 80^\circ$ and $\Psi = 8.5^\circ$ [58].

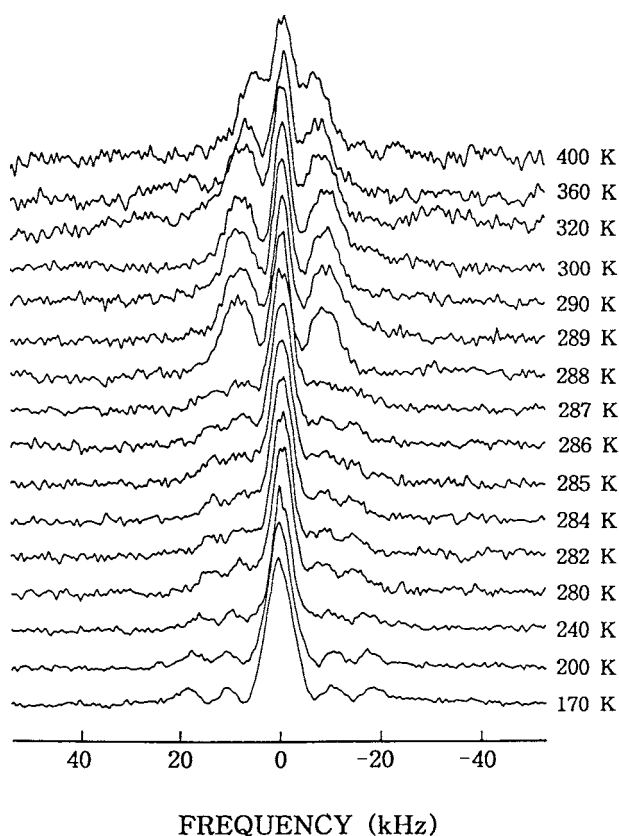


Figure 7. The temperature dependence of the ${}^7\text{Li}$ NMR spectra in the LiNH_4SO_4 crystal.

The three-line structure is a result of the quadrupole interaction of the ${}^7\text{Li}$ ($I = 3/2$) nucleus. However, two different groups of Li resonances were recorded in phase III, originating from Li(I) and Li(II), respectively. These two signals are associated with two physically inequivalent positions of lithium atoms in the unit cell. The rotation pattern of Li(I) and Li(II) was measured in three crystallographic planes below 287 K. Here, the signal for Li(II) showed very strong intensity, while the Li(I) showed very weak intensity. Two different Li resonance groups with different magnitudes of quadrupole splitting were analysed. At 200 K, the quadrupole coupling constant and asymmetry parameter were determined as 25.5 kHz and 0.33 for Li(I), 34 kHz and 0.88 for Li(II), respectively. The principal axes of the EFG tensor at low temperatures were not the same as those obtained above T_c . The principal axes X , Y and Z of the EFG tensor lie along the Eulerian angles $\Phi = 90^\circ$, $\Theta = 90^\circ$, $\Psi = 0^\circ$ and $\Phi = 70^\circ$, $\Theta = 87^\circ$, $\Psi = 79^\circ$, for Li(I) and Li(II), respectively. The EFG tensors of Li(I) and Li(II) are both asymmetric, and the orientations of the principal axes of the EFG tensors also do not coincide for Li(I) and Li(II) [57].

The temperature dependences of e^2qQ/h and η are shown in figure 8. In the temperature range 170 to 400 K, which includes the II–III phase transition, there is an abrupt change in the parameters of ${}^7\text{Li}$ NMR. This means that the phase transition is first order. At the transition point of 287 K, the ${}^7\text{Li}$ NMR line splits into two sets. Below 287 K, the quadrupole parameter of Li(I) slowly increases as the temperature decreases, while that of Li(II) was found to drastically

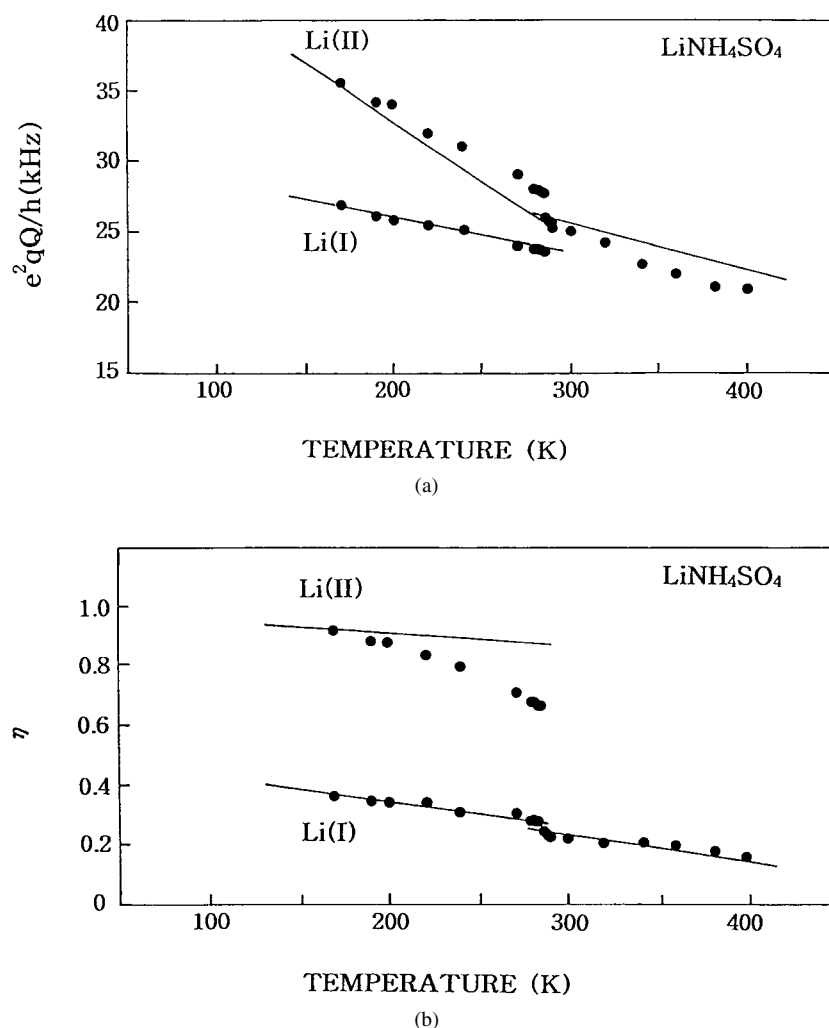


Figure 8. Temperature dependence of the nuclear quadrupole coupling constant and asymmetry parameter for ${}^7\text{Li}$ NMR in the LiNH_4SO_4 crystal.

increase with the temperature. The moment of inertia calculated from the crystal structure is $I_x = 2.56 \times 10^{-45} \text{ kg m}^2$ for the X -axis. The solid lines above 287 K are the predicted values of e^2qQ/h and η with $w_x = 1.60 \times 10^{13} \text{ rad s}^{-1}$ for Li. Below 287 K, the values of e^2qQ/h and η are $w_x = 1.60 \times 10^{13} \text{ rad s}^{-1}$ and $w_x = 1.03 \times 10^{13} \text{ rad s}^{-1}$ for Li(I) and Li(II), respectively.

5. Discussion and conclusion

The ${}^7\text{Li}$ NMR in the single crystal form of LiXSO_4 ($X = \text{K, Rb, Cs and NH}_4$) grown by the slow evaporation method has been investigated by employing a Bruker FT NMR spectrometer. From the experimental data, the quadrupole coupling constant, asymmetry parameter and the direction of EFG tensor were determined as functions of temperature. The nuclear electric quadrupole interaction of the ${}^7\text{Li}$ nucleus having the nuclear spin $I = 3/2$ provides information

about the electric field gradient produced by ions surrounding the resonant nucleus. Thus, the quadrupole coupling constant and asymmetry parameter of ${}^7\text{Li}$ reveal the configuration of ionic charges around the Li^+ . The e^2qQ/h values for the ${}^7\text{Li}$ nucleus in the LiXSO_4 crystal system were found to be similar to each other. This similarity is consistent with the fact that LiXSO_4 single crystals have isomorphous structures. The differences in the field gradient in the case of each crystal were observed at different positions of the Li ions. The splitting of ${}^7\text{Li}$ NMR spectra at T_c demonstrates the occurrence of a phase transition which is connected with a lowering of the Li^+ site symmetry and also indicates the formation of ferroelastic domains.

From the NMR of ${}^7\text{Li}$ in LiXSO_4 , we can observe the mechanism of phase transitions. In the case of LiKSO_4 and LiNH_4SO_4 crystals, the NMR parameter shows a discontinuity at T_c . This means that the phase transition is a first-order transition. Also, the parameters of the LiCsSO_4 crystal show continuity at T_c , and undergo a second-order phase transition.

Meng and Cao [46] have made a ${}^7\text{Li}$ NMR analysis of LiKSO_4 at room temperature. According to their results, the rotation pattern in the ab -plane was angle independent, while the rotation patterns in the ac - and bc -plane were angle dependent. The above result indicates that the electric field gradient tensors of ${}^7\text{Li}$ were axially symmetric. However, the ${}^7\text{Li}$ NMR parameter in LiKSO_4 crystals studied by our results were non-axially symmetric. This result is not consistent with the result of other groups. Consequently, LiKSO_4 single crystals may have different crystal structures according to the conditions of crystal growth.

The proposed torsional angular frequencies in LiXSO_4 single crystals were determined from the temperature dependent quadrupole parameters. Based on these results, the differences in atomic weight of X in the LiXSO_4 single crystals are responsible for the differences in the torsional angular frequencies.

Acknowledgment

This work was supported by the Korean Physical Society (1999).

References

- [1] Kruglik A I, Misyul S V and Simonov M A 1979 *Sov. Phys. Crystallogr.* **24** 333
- [2] Mashiyama H, Hasebe K, Tanisaki S, Shiroishi Y and Sawada S 1979 *J. Phys. Soc. Japan* **47** 1198
- [3] Kruglik A I, Simonov M A, Zhelezin E P and Belov N V 1979 *Sov. Phys.–Dokl.* **24** 596
- [4] Tanisaki S, Mashiyama H, Hasebe K, Shiroishi Y and Sawada S 1980 *Acta Crystallogr. B* **36** 3084
- [5] Pietraszko A, Tomaszewski P E and Lukaszewicz K 1981 *Phase Transitions* **2** 141
- [6] Pura B and Przedmojski J 1981 *Acta Phys. Pol. A* **59** 785
- [7] Tomaszewski P E and Lukaszewicz K 1982 *Phys. Status Solidi a* **71** k53
- [8] Sandomirskii P A, Meshalkin S S and Rozhdestvenskaya I V 1983 *Sov. Phys.–Crystallogr.* **28** 33
- [9] Tomaszewski P E and Lukaszewicz K 1983 *Phase Transitions* **4** 37
- [10] Karppinen M, Lundgren J O and Liminga R 1983 *Acta Crystallogr. C* **39** 34
- [11] Tamhane S B, Sequeira A and Chidambaram R 1984 *Acta Crystallogr. C* **40** 1648
- [12] Schulz H, Zucker U and Frech R 1985 *Acta Crystallogr. B* **41** 21
- [13] Klapper H, Hahn T and Chung S J 1987 *Acta Crystallogr. B* **43** 147
- [14] Asahi T and Hasebe K 1988 *J. Phys. Soc. Japan* **57** 4184
- [15] Tomaszewski P E 1992 *Solid State Commun.* **81** 333
- [16] Rao T R, Bansal M L, Sahni V C and Roy A P 1976 *Phys. Status Solidi b* **75** k31
- [17] Bansal M L, Deb S K, Roy A P and Sahni V C 1980 *Solid State Commun.* **36** 1047
- [18] Teeters D and Frech R 1982 *Phys. Rev. B* **26** 4132
- [19] Teeters D and Frech R 1982 *Phys. Rev. B* **26** 5897
- [20] Ramakrishnan V, Nayar V U and Aruldas G 1985 *Infrared Phys.* **25** 607
- [21] Oliveira A J, Germano F A, Filho J M, Melo F E A and Moreira J E 1988 *Phys. Rev. B* **38** 12 633
- [22] Farhi R and Coudin F 1989 *J. Phys.: Condens. Matter* **1** 6951

- [23] Lemos V, Gomes P A P, Melo F E A, Filho J M and Moreira J E 1989 *J. Raman Spectrosc.* **20** 155
- [24] Morell G, Devanarayanan S and Katiyar R S 1991 *J. Raman Spectrosc.* **22** 529
- [25] Martins A R M, Germano F A, Filho J M, Melo F E A and Moreira J E 1991 *Phys. Rev. B* **44** 6723
- [26] Lemos V, Camargo F, Hernandez A C and Freire P T C 1993 *J. Raman Spectrosc.* **24** 133
- [27] Shashikala M N, Chandrabhas N, Jayaram K, Jayaraman A and Sood A K 1994 *J. Phys. Chem. Solids* **55** 107
- [28] Hossain M A, Srivastava J P, Khulbe P K, Menon L and Bist H D 1994 *J. Phys. Chem Solids* **55** 85
- [29] Poulet H and Mathieu J P 1977 *Solid State Commun.* **21** 421
- [30] Holuj F and Drozdowski M 1981 *Ferroelectrics* **36** 379
- [31] Fonseca C H A, Ribeiro G M, Gazzinelli R and Chaves A S 1983 *Solid State Commun.* **46** 221
- [32] Yu J T, Kou J M, Huang S J and Co L S 1986 *J. Phys. Chem. Solids* **47** 121
- [33] Huang S J and Yu J T 1987 *Solid State Commun.* **63** 745
- [34] Murthy K and Bhat S V 1988 *J. Phys. C: Solid State Phys.* **21** 597
- [35] Tsu Y J 1988 *J. Phys. C: Solid State Phys.* **21** 759
- [36] Yu J T, Chou S Y and Huang S J 1988 *J. Phys. Chem. Solids* **49** 289
- [37] Tsai S F and Yu J T 1988 *J. Phys. Soc. Japan* **57** 2540
- [38] Morais P C, Ribeiro G M and Chaves A S 1989 *Solid State Commun.* **52** 291
- [39] Misra S K and Misiak L E 1993 *Phys. Rev. B* **48** 13 579
- [40] Chou S Y, Yu J T, Wu C J and Jeng Y H 1993 *Solid State Commun.* **88** 149
- [41] Rao Y S and Sunandana C S 1994 *J. Phys. Chem. Solids* **55** 605
- [42] Yuzvak V I, Zhrebtsova I, Shkuryaeva V B and Aleksandrova I P 1975 *Sov. Phys. Crystallogr.* **19** 480
- [43] Aleksandrov K S, Aleksandrova I P, Anistratov A T and Shabanov V E 1977 *Izv. Akad. Nauk. SSSR. Ser. Fiz.* **41** 599
- [44] Aleksandrova I P, Kabanov I S, Melnikova S V, Chekmasova T I and Yuzvak V I 1977 *Sov. Phys. Solid State* **19** 605
- [45] Shenoy R K and Ramakrishna K 1980 *J. Phys. C: Solid State Phys.* **13** 5429
- [46] Meng Q A and Cao Q J 1982 *Acta Phys. Sin.* **31** 1045
- [47] Holuj F 1985 *Ferroelectrics* **65** 55
- [48] Holuj F 1986 *Ferroelectrics* **67** 103
- [49] Topic B, Haeberlen U and Blinc R 1988 *Z. Phys. B* **70** 95
- [50] Lim A R, Choh S H and Jeong S Y 1996 *J. Phys.: Condens. Matter* **8** 4597
- [51] Lim A R, Hong K S, Choh S H and Jeong S Y 1997 *Solid State Commun.* **103** 693
- [52] Lim A R and Jeong S Y 1997 *Phys. Status Solidi b* **201** 285
- [53] Lim A R, Park S H and Choh S H 1997 *J. Phys.: Condens. Matter* **9** 4755
- [54] Lim A R and Jeong S Y 1998 *J. Phys.: Condens. Matter* **10** 9841
- [55] Lim A R and Jeong S Y 1999 *J. Phys. Chem. Solids* **60** 1773
- [56] Lim A R, Han T J and Jeong S Y 1999 *Phys. Status Solidi b* **214** 375
- [57] Lim A R, Choh S H and Jeong S Y 1999 *J. Phys.: Condens. Matter* **11** 8141
- [58] Lim A R, Park S E and Jeong S Y 2000 *Solid State Commun.* **113** 389
- [59] Ivanov N R 1985 *Ferroelectrics* **64** 13
- [60] Sorge G and Hempel H 1986 *Phys. Status Solidi a* **97** 431
- [61] Kleemann W, Schafer F J and Chaves A S 1987 *Solid State Commun.* **64** 1001
- [62] Czajkowski M, Drozdowski M and Kozielski M 1988 *Phys. Status Solidi a* **110** 437
- [63] Ganot F, Farhi R, Dugautier C and Moch P 1989 *Phys. Rev. B* **40** 273
- [64] Ortega J, Etxebarria J and Breczewski T J 1993 *Appl. Cryst.* **26** 549
- [65] Lim A R and Park S H 1997 *Phys. Status Solidi b* **163** 59
- [66] Lim A R and Jeong S Y 1997 *Phys. Status Solidi a* **164** 673
- [67] Lim A R and Jeong S Y 1998 *J. Phys. D: Appl. Phys.* **31** 453
- [68] Lim A R and Jeong S Y 1998 *Phys. Status Solidi b* **207** 81
- [69] Aizu K 1969 *J. Phys. Soc. Japan* **27** 387
- [70] Krajewski T, Breczewski T, Piskunowicz P and Mroz B 1985 *Ferroelectr. Lett.* **4** 95
- [71] Pimenta M A, Echegut P, Luspini Y, Hauret G, Gervais F and Abelard P 1989 *Phys. Rev. B* **39** 3361
- [72] Chung S J and Hahn T 1972 *Acta Crystallogr. A* **28** s57
- [73] Lim A R and Jeong S Y 2000 *Solid State Commun.* **116** 231
- [74] Bayer H Z 1951 *Physik* **130** 227
- [75] Wang T C 1955 *Phys. Rev.* **99** 566
- [76] Shiroishi Y, Nakata A and Sawada S 1976 *J. Phys. Soc. Japan* **40** 911
- [77] Shiroishi Y and Sawada S 1979 *J. Phys. Soc. Japan* **46** 148
- [78] Mashiyama H and Unruh H G 1985 *J. Phys. Soc. Japan* **54** 822

- [79] Kunishige A, Izumi T and Sawada S 1986 *J. Phys. Soc. Japan* **55** 2469
- [80] Kunishige A and Mashiyama H 1987 *J. Phys. Soc. Japan* **56** 3189
- [81] Yamaguchi T and Sawada S 1980 *Proc. JSSF-2 (Kyoto) J. Phys. Soc. Japan* **49** 81
- [82] Chary B R, Bhat H L, Chandrasekhar P and Narayanan P S 1985 *Pramana* **24** 545
- [83] Pepinsky R, Vedam K and Hoshino S 1958 *Phys. Rev.* **111** 1467
- [84] Simonson T, Denoyer F and Moret R 1984 *J. Physique* **45** 1257
- [85] Itoh K, Ishikura H and Nakamura E 1969 *Acta Crystallogr. B* **25** 2298
- [86] Dollase W A 1969 *Acta Crystallogr. B* **25** 2298
- [87] Kruglik A I, Simobnov M A and Alesandrov K S 1978 *Sov. Phys.-Crystallogr.* **23** 274